



Green Synthesis of Silver Nanoparticles Using *Mesua ferrea* Extract for Anti-Bacterial Activity

Manoj Kumar*, Mr. Pramod Kumar, Mr. Pradeep Yadav

Shri Ramnath Singh Institute of Pharmaceutical Science and Technology, Sitholi, Gwalior (M.P.). India.

Received: 09 February 2026

Revised: 28 February 2026

Accepted: 10 March 2026

ABSTRACT

In this work, a green and environmentally friendly production of silver nanoparticles (AgNPs) utilizing *Mesua ferrea* extract is reported, and their physicochemical properties and antibacterial activity against certain Gram-negative foodborne pathogens are assessed. *Mesua ferrea* aerial parts' aqueous extract demonstrated moderate antioxidant activity and a high phenolic content, confirming its usefulness as a reducing and capping agent. AgNPs were effectively produced under ideal circumstances, which included adjusting the pH, extract concentration, and microwave irradiation to regulate the size and form of the particles. FTIR research demonstrated the role of phytochemicals such as phenols, flavonoids, and alkaloids in nanoparticle stabilization, whereas UV-visible spectroscopy using surface plasmon resonance validated the synthesis of AgNPs. The spherical shape, nanoscale size, and crystalline structure of the AgNPs were verified by XRD studies. Good colloidal stability and homogenous particle dispersion were shown by DLS and zeta potential studies. Disk diffusion, MIC, MBC, and time-kill tests were used to assess the antibacterial activity of the produced AgNPs against *Escherichia coli*, *Klebsiella pneumoniae*, *Salmonella Typhimurium*, and *Salmonella Enteritidis*. With low MIC and MBC values and significant, broad-spectrum antibacterial activity, the AgNPs demonstrated efficient bactericidal action in a brief exposure period. Overall, this work demonstrates the potential of AgNPs mediated by *Mesua ferrea* as stable, efficient, and environmentally safe antibacterial agents with intriguing uses in the realms of biomedicine and food safety.

Keywords: Nanotechnology, Silver nanoparticles, *Mesua ferrea*, antibacterial

INTRODUCTION

As an environmentally acceptable substitute for traditional physical and chemical techniques of nanoparticle production, the development of green nanotechnology has attracted a lot of interest. [1] Due to their distinct physicochemical characteristics and broad-spectrum antibacterial action, silver nanoparticles (AgNPs) have garnered significant attention among other metal nanoparticles. [2] Conventional synthesis techniques can result in dangerous byproducts, excessive energy usage, and poisonous compounds. [3] On the other hand, phytochemicals found in plant extracts function as natural reducing, stabilizing, and capping agents in plant-mediated green synthesis, which provides a straightforward, economical, and sustainable method. This method improves the biological compatibility of the produced nanoparticles while reducing their negative effects on the environment. [4]

The medicinal plant *Mesua ferrea*, which is abundant in bioactive substances including terpenoids, phenolics, and flavonoids, has demonstrated great promise for the production of green nanoparticles. [5] These phytochemicals both inhibit aggregation and aid in the reduction of silver ions into stable silver nanoparticles. [6, 7] The green synthesis of AgNPs using *Mesua ferrea* extract and the assessment of their antibacterial effectiveness against certain pathogenic bacteria are the main objectives of this work. This effort intends to generate efficient AgNPs with higher antibacterial activity by optimizing synthesis conditions and using an ecologically friendly approach. This will contribute to alternate tactics for fighting microbial illnesses and antibiotic resistance.

MATERIALS AND METHODS

Collection of Materials: Fresh leaves, stem and flower of *Mesua ferrea* plant was collected from Gwalior district, during the month of February 2024. The plant was identified by Taxonomist, Department of Botany, and deposited in the herbarium.

Extraction of *Mesua ferrea*: To enhance the surface area for more effective extraction, the aerial sections of *Mesua ferrea* were first fully dried and then finely pulverized. Five grams of this powdered substance were added to a sterile flask that held one hundred milliliters of distilled water. To promote the best extraction of water-soluble bioactive chemicals, the mixture was heated in a water bath at 70°C for 45 minutes. A clear aqueous extract was produced when the mixture was heated, cooled to room

temperature, and filtered using Whatman No. 1 filter paper to get rid of plant debris. Before being used in the manufacture of silver nanoparticles or other analyses, the filtrate was carefully collected, moved to an airtight container to avoid contamination and evaporation, and kept at 4°C to preserve the phytochemicals and prevent microbial development. [8, 9]

Preliminary Phytochemical Screening: The extract of *Mesua ferrea* was subjected to a preliminary phytochemical screening to identify the active chemical constituents like alkaloids, glycosides, saponins, steroids, tannin and phenolic compound. [10]

Green Synthesis of Silver Nanoparticles

Synthesis of Silver Nanoparticles: After adding 5.0 mL of 10 mM AgNO₃ solution and 5.0 mL of *Mesua ferrea* extract to a 50 mL flask, add 0.5 mL of a 25% ammonia solution and fill the flask to capacity with deionized water. [11]

Synthesis of Ag Octahedron and Tetrahedron: A 10 mL volumetric flask containing *Mesua ferrea* extract was filled with around 20 mg of precisely weighed silver nitrate (AgNO₃) and 0.5 mL of 25% ammonia solution. In a different formulation, 10 mL of *Mesua ferrea* extract and 0.5 mL of 25% ammonia solution were mixed with 20 mg of AgNO₃. One milliliter of pre-synthesised silver nanoparticles was then added. In a different formulation, 10 mL of *Mesua ferrea* extract and 2 mL of 0.1 M NaOH solution were combined with 20 mg of AgNO₃. For a maximum of 133 seconds, all reaction mixtures were exposed to microwave radiation at 750 W in a micro-oven. Following irradiation, a 0.3 mL aliquot from each reaction mixture was diluted with 2.2 mL of deionized water, and the resulting solutions were used for UV–Visible spectrophotometric analysis. [12]

Characterization of AgNPs: UV-visible spectrophotometry (Shimadzu UV-2550, Japan) was used to track the biogenesis of silver (Ag) and gold (Au) nanoparticles. All spectra were adjusted against deionized (DI) water as a background. To verify the creation of nanoparticles, the reduction reaction's progress and the emergence of surface plasmon resonance bands were observed over a variety of pH values and time intervals. The functional groups involved in the reduction, capping, and stability of silver nanoparticles made with *Mesua ferrea* were identified using Fourier Transform Infrared (FTIR) spectroscopy (Perkin Elmer FTIR spectrophotometer). Dried nanoparticles were finely crushed, combined with spectroscopic-grade KBr, and compressed into pellets for FTIR measurement. To detect biomolecules interacting with the surface of the nanoparticle, spectra were acquired in the 4000–400 cm⁻¹ region at a resolution of 4 cm⁻¹. [13, 14]

X-ray diffraction (XRD) investigation utilizing a Bruker AXS D8 Advance diffractometer with Cu K α radiation ($\lambda = 1.5406 \text{ \AA}$), scanned across a 2θ range of 10–90°, further verified the crystalline character of the nanoparticles. The Debye-Scherrer equation was used to determine the size of crystallites. A Zetasizer Nano ZS (Malvern Instruments, UK) was used to test the polydispersity index and particle size distribution, and the same device was used to measure the zeta potential and evaluate surface charge and colloidal stability. To guarantee accuracy and repeatability, samples were suitably diluted and average results were computed from three separate measurements. [15, 16]

Antibacterial Activity: The biosynthesized silver nanoparticles' (AgNPs) antibacterial activity was assessed against a few Gram-negative foodborne pathogens. The American Type Culture Collection provided all of the bacterial strains, which were cultivated in Mueller Hinton broth (MHB) at 37 °C for 24 hours while being continuously shaken at 200 rpm. Resazurin salt was dissolved in distilled water to create a resazurin solution (0.02% w/v), which was then filtered through a 0.2 μm membrane filter and kept at 4 °C for up to two weeks. Initially, bacterial lawns were created on Mueller Hinton agar (MHA) plates using the Kirby–Bauer disk diffusion technique for antibacterial screening. The agar surface was covered with sterile disks containing *Mesua ferrea* extract, silver nitrate solution (1 mM), and green-synthesized AgNPs. The disks were then incubated for 24 hours at 37 °C. The zones of inhibition surrounding the disks were measured in order to evaluate the antibacterial effectiveness. [17]

Using the broth microdilution technique on 96-well microtiter plates, the minimum inhibitory concentration (MIC) and minimum bactericidal concentration (MBC) of the produced AgNPs were calculated in accordance with CLSI (2012) criteria. Twofold successive dilutions of AgNPs (beginning at 500 $\mu\text{g/mL}$) were produced in MHB, and bacterial inocula were standardized to 10⁶ CFU/mL. The plates were incubated at 37 °C for 24 hours after the resazurin indicator was added, and color changes were monitored to assess bacterial growth. While the MBC was determined by subculturing samples onto MHA plates and finding the lowest concentration exhibiting no discernible growth, the MIC was defined as the lowest concentration that prevented color change, suggesting growth inhibition. Furthermore, bacterial cultures were exposed to various multiples of MIC (0–8 \times MIC) and incubated at 37 °C with shaking in order to perform time-kill tests. To assess the bactericidal kinetics of AgNPs, samples were taken at predetermined intervals, plated on MHA, and colony counts were calculated during a 24-hour incubation period. [18]

RESULTS AND DISCUSSION

Evaluation of Extract: The decoction procedure yielded an aqueous extract of *Mesua ferrea*'s aerial parts (leaves, stem, and flowers) that had a yellowish-brown hue, a greasy texture, and a vague odor. It was discovered that the extract was insoluble in acidic solutions but soluble in alcohol and water. The extraction technique produced a practical yield of 4.11 g, or 4.11% w/w.

Pre-Phytochemical Analysis: Several bioactive groups were found in the aqueous aerial component extract of *Mesua ferrea*, according to the first phytochemical screening. Dragendorff's, Mayer's, and Wagner's assays yielded positive findings for alkaloids, whilst Hager's reagent produced negative results. A positive Keller-Kiliani test revealed the presence of glycosides. Hemolytic and foam tests were negative, indicating the absence of saponins. The Liebermann-Burchard test revealed a positive result, suggesting the presence of certain steroidal components, whereas the Salkowski test revealed a negative result among steroids. Positive reactions with ferric chloride and lead acetate demonstrated the presence of tannins and phenolic chemicals. A positive Shinoda test also revealed the presence of flavonoids.

Green Synthesis and Characterization of Silver Nanoparticles: *Mesua ferrea* extract was used as a capping and reducing agent in the environmentally friendly manufacture of silver nanoparticles. This plant extract has been effectively used for the environmentally friendly production of many metal oxides, such as iron oxide, indium oxide, and hydroxyapatite, in addition to silver nanoparticles. The current work highlights the application of *Mesua ferrea* for microwave-assisted synthesis to precisely regulate nanoparticle size and shape, as well as to investigate hitherto unexplored biological activities, including antibacterial properties, despite the existence of some preliminary investigations. By modifying the extract concentration, metal salt concentration, reaction temperature, and pH, the synthesis parameters were tuned. The emergence of a yellow hue caused by surface plasmon resonance, which became more intense with time, was indicative of the creation of silver nanoparticles. UV-Visible spectroscopy was employed to monitor nanoparticle growth, while control experiments using deionized water showed no color change, confirming the crucial role of the plant extract.

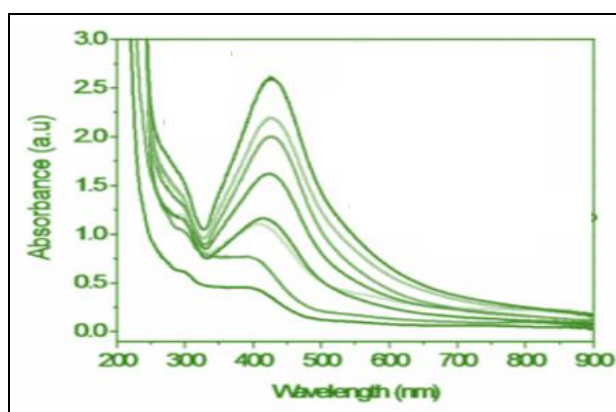


Figure 1: UV-Visible spectrum of continuous growth of Ag nanoparticles using *Mesua ferrea* different time intervals of AgNPs (30 min, 1, 2, 3, 4, 6, 12 & 24 h)

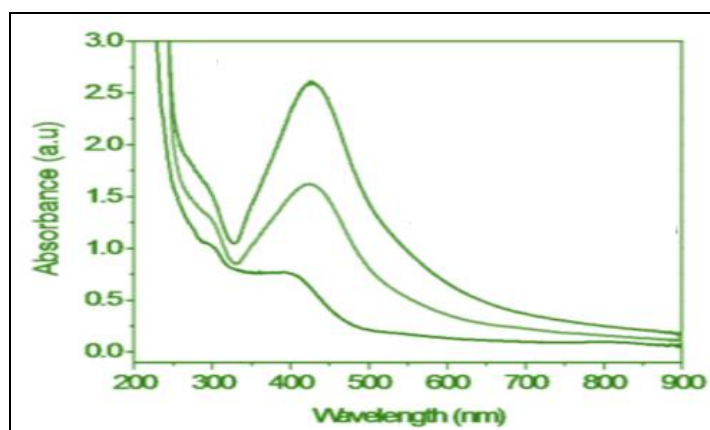


Figure 2: UV-Visible spectrum of continuous growth of Ag nanoparticles using *Mesua ferrea* different concentration of extract (1.0, 2.5 and 5.0 mL at pH 11.25).

Synthesis of silver nanoparticles: It is commonly known that UV-visible spectroscopy is a useful method for analyzing the size and form of nanoparticles in aqueous solutions. In this work, UV-visible spectra were recorded at various intervals to track the production of silver nanoparticles. Important details about the nucleation, growth, and morphological evolution of the silver nanoparticles during the synthesis process were revealed by changes in absorbance and the emergence of distinctive surface plasmon resonance bands.

Table 1: Synthesis of silver nanoparticles with varying concentration of extract.

| Sample ID | Volume of Extract (mL) | Volume of 10 mM AgNO ₃ (mL) | Volume of Water (mL) |
|-----------|------------------------|--|----------------------|
| MS1 | 1.0 | 5.0 | 44.0 |
| MS2 | 2.5 | 5.0 | 42.5 |
| MS3 | 5.0 | 5.0 | 40.0 |

FT-IR Spectroscopic Analysis: The biomolecules involved in the reduction, capping, and stability of the produced silver nanoparticles were identified using FTIR spectroscopy analysis, as seen in Figure 3. The aqueous *Mesua ferrea* extract's FTIR spectra showed moderate absorption peaks at 2128.02, 1665, 1281.36, and 1053 cm⁻¹, as well as significant peaks at 3369.09 and 1620.55 cm⁻¹. Alcohols and phenolic chemicals, most likely produced from plant enzymes and polysaccharides, are indicated by the large peak at 3369.09 cm⁻¹ and the band at 1503 cm⁻¹, which correspond to O–H stretching vibrations of hydrogen-bonded hydroxyl groups. Peaks at 2937 and 1407.73 cm⁻¹ are attributed to O–H stretching vibrations of carboxylic acids, while the bands at 2128.02 and 1620.55 cm⁻¹ correspond to C=C stretching vibrations of alkenes. The presence of aromatic amines is suggested by C–N stretching vibrations. In the FTIR spectrum of the synthesized silver nanoparticles, a broad absorption band at 3338.61 cm⁻¹ was observed, which is characteristic of O–H stretching vibrations of alcohol groups, along with a strong band at 1634.19 cm⁻¹ corresponding to C=C stretching. The active participation of phytochemicals like flavonoids, phenols, alkaloids, terpenoids, and tannins is confirmed by the decrease in intensity of peaks at 2937.96, 2128.02, 1407.73, 1281.36, 1103.23, 997.52, 926.62, and 597.14 cm⁻¹, as well as discernible shifts in peaks at 3369.09, 1620.55, and tannins. These biomolecules, which have hydroxyl, amino, and unsaturated functional groups, are essential for both the efficient capping and stability of the produced silver nanoparticles and the reduction of silver ions.

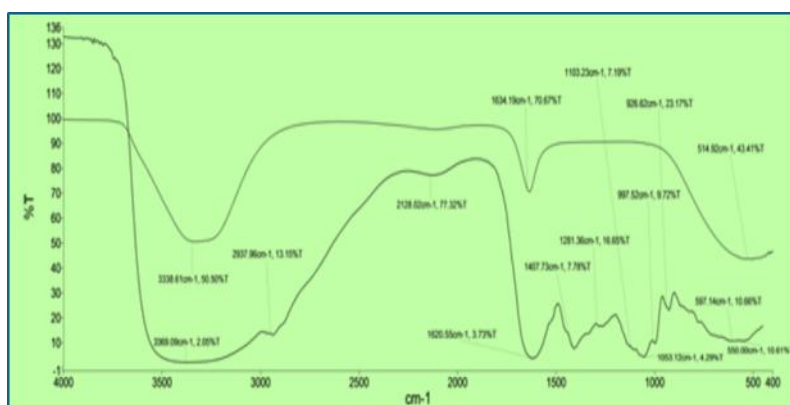


Figure 3: FTIR Spectrum of Silver Nanoparticles Synthesized from *M. ferrea*

XRD Analysis: Figure 4 shows the X-ray diffraction (XRD) pattern of the silver nanoparticles made using *Mesua ferrea* extract. According to JCPDS file No. 03-0921, the diffraction peaks were indexed to the (111), (200), (220), and (311) planes, which correspond to the face-centered cubic (fcc) structure of silver nanoparticles. The peaks' observed widening suggests that the particles are nanocrystalline. All things considered, the XRD data strongly support the creation of silver nanoparticles, supporting the findings of UV-visible spectroscopy.

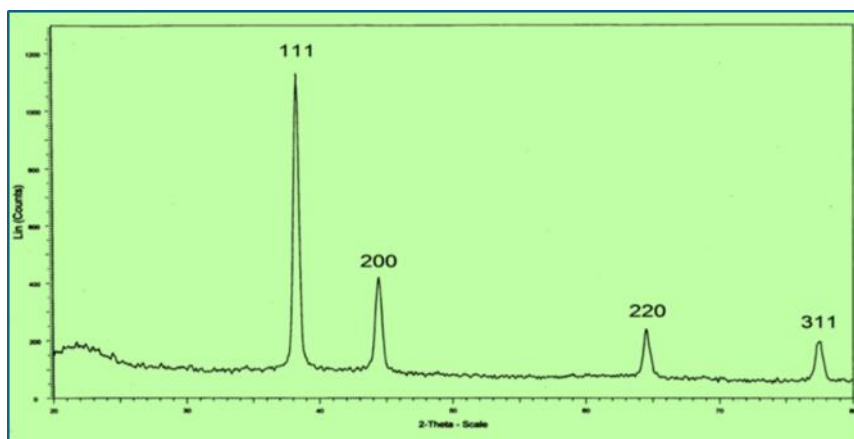


Figure 4: The XRD pattern of Ag nanoparticles synthesized using extract

Mean Particle Size, Polydispersity Index (PDI), and Zeta Potential of *Mesua ferrea* Silver Nanoparticles: The hydrodynamic size, particle dispersion, and surface charge of the green-synthesised silver nanoparticles were assessed using Dynamic Light Scattering (DLS) methodology. The *Mesua ferrea*-mediated AgNPs are tiny, evenly dispersed, and extremely stable, which makes them attractive options for antibacterial and biomedical applications, according to the DLS and zeta potential studies. Particle stability and possible biological activity are both improved by the presence of bioactive plant metabolites. The following is a summary of the findings:

Table 2: The mean particle size, polydispersity index and zeta potential

| Parameter | Value |
|----------------------------|---------------|
| Mean particle size (nm) | 153.1±2.42 |
| Polydispersity index (PDI) | 0.121±0.081 |
| Zeta potential (mV) | +52.1±3.11 mV |

Biological Evaluation: Table 3 summarizes the antibacterial activity of the produced AgNPs as determined by disk diffusion, MIC, and MBC tests. The development of distinct inhibition zones surrounding the AgNP-impregnated disks in the disk diffusion testing demonstrated their potent antibacterial efficacy against the examined Gram-negative foodborne pathogens. Further quantitative evaluation of antibacterial effectiveness was carried out utilizing MIC and MBC measurements, since the disk diffusion method functions as an initial screening approach (Burt, 2004). AgNPs had MIC values ranging from 3.9 to 7.8 µg/mL, with *K. pneumoniae*, *S. Typhimurium*, and *S. Enteritidis* showing greater sensitivity at 3.9 µg/mL and *E. coli* showing a relatively higher MIC of 7.8 µg/mL. These results were corroborated by the MBC values, which showed total bacterial death at 3.9 µg/mL for *K. pneumoniae* as well as *S. Enteritidis*, whereas *S. Typhimurium* and *E. coli* have a lipopolysaccharide-rich outer membrane that might impede nanoparticle interaction by trapping or blocking the positively charged AgNPs, which may explain their reduced susceptibility to AgNPs. Overall, our findings show that green-synthesised AgNPs have a high antibacterial potential against Gram-negative foodborne pathogens.

Table 3: The diameter of zone inhibition (mm), MIC value (µg/mL), and MBC value (µg/mL).

| Bacteria | Diameter of Inhibition Zone (mm) | MIC (µg/mL) | MBC (µg/mL) |
|-------------------------------|----------------------------------|-------------|-------------|
| <i>Escherichia coli</i> | 15 | 7.8 | 7.8 |
| <i>Klebsiella pneumoniae</i> | 10 | 3.9 | 3.9 |
| <i>Salmonella Typhimurium</i> | 20 | 3.9 | 7.8 |
| <i>Salmonella Enteritidis</i> | 20 | 3.9 | 3.9 |

The time-kill kinetics of the four pathogenic pathogens. With a decrease of $\geq 3 \log_{10}$ CFU/mL (about 99%), the produced AgNPs demonstrated high bactericidal activity against all tested Gram-negative bacteria, confirming their efficient killing capacity. After two hours of exposure, full bactericidal action was seen for *E. coli* at 4× MIC (31.2 µg/mL) and 8× MIC (62.4 µg/mL). At lower quantities of *K. pneumoniae*, such as 2× MIC (7.8 µg/mL), 4× MIC (15.6 µg/mL), and 8× MIC (31.2 µg/mL), bacterial eradication was accomplished in 2 hours. At 4× MIC (15.6 µg/mL) and 8× MIC (31.2 µg/mL), *S. Typhimurium* demonstrated faster susceptibility, with total bacterial death taking place in 1 hour. For *S. Enteritidis*, a quicker killing effect was shown within

1 hour at $8\times$ MIC (31.2 $\mu\text{g/mL}$), but the bactericidal endpoint was achieved after 2 hours at $2\times$ MIC (7.8 $\mu\text{g/mL}$) and $4\times$ MIC (15.6 $\mu\text{g/mL}$). AgNPs have broad-spectrum antibacterial activity and similar bactericidal effects against all Gram-negative foodborne bacteria examined, according to statistical analysis that showed no significant differences ($P > 0.05$) among the tested pathogens.

CONCLUSION

To sum up, our study effectively shows that *Mesua ferrea* aqueous extract may be used for the environmentally friendly manufacture of stable silver nanoparticles. The produced AgNPs show promise as substitute antimicrobial agents due to their regulated size, crystallinity, and strong antibacterial activity against Gram-negative organisms. Additionally, this work highlights the dual function of phytochemicals originating from plants as capping and reducing agents, opening the door for the creation of eco-friendly nanomaterials with biological uses.

REFERENCES

1. Castellano J.J., Shafii S.M., Ko F., Donate G., Wright T.E., Mannari R.J., Payne W.G., Smith D.J., Robson M.C. Comparative evaluation of silver-containing antimicrobial dressings and drugs. *Int. Wound J.* 2007;4:114–122. doi: 10.1111/j.1742-481X.2007.00316.x.
2. Kim Y.T., Kim K., Han J.H., Kimmel R.M. Antimicrobial Active Packaging for Food. *Smart Packag. Technol. Fast Mov. Consum. Goods.* 2008;76:99–110. doi: 10.1002/9780470753699.ch6.
3. Kampmann Y., De Clerck E., Kohn S., Patchala D.K., Langerock R., Kreyenschmidt J. Study on the antimicrobial effect of silver-containing inner liners in refrigerators. *J. Appl. Microbiol.* 2008;104:1808–1814. doi: 10.1111/j.1365-2672.2008.03727.x.
4. Kędziora A., Speruda M., Krzyżewska E., Rybka J., Łukowiak A., Bugła-Płoskońska G. Similarities and differences between silver ions and silver in nanoforms as antibacterial agents. *Int. J. Mol. Sci.* 2018;19:444. doi: 10.3390/ijms19020444.
5. Garg S, Kameshwar S, Rajeev R, Pankaj A, Parshuram M. In- vivo Antioxidant activity and hepatoprotective effects of methanolic extracts of *Mesua ferrea* L. *Int J Pharmatechnol Res.* 2009;(1):1692-96.
6. Makchuchit S, Itharat A, Tewtrakul S. Antioxidant and Nitric Oxide Inhibition activities of Thai Medicinal Plants. *J Med Assoc Thai.* 2010;(93):227-35.
7. Hassan TM, Ali MS, Alimuzzaman M, Raihan SZ. Analgesic activity of *Mesua ferrea* Linn. *Dhaka Univ. J Pharm Sci.* 2006;(5):73-5.
8. Gopalakrishnan C, Shankarnarayanan D, Nazimudeen SK, Viswanathan S, Kameswaran L. Anti-inflammatory and CNS depressant activities of xanthenes from *Calophyllum inophyllum* and *Mesua ferrea*. *Ind J Pharmacol.* 1980;(12):181-91.
9. Subramanyum RM. NV subba roolate fatty acid composition of nahor (*Mesua Ferrae* Linn) seed oil. *J Richer Imagerie Med.* 1977;(12):97-9.
10. Prashanth KV, Chauhan NS, Padh H, Rajani M. Search for antibacterial and anti fungal agents from selected indian medicinal plant. *J Ethnopharmacol.* 2006;(107):182-8.
11. Siddiqi K.S., Husen A., Rao R.A.K. A review on biosynthesis of silver nanoparticles and their biocidal properties. *J. Nanobiotechnol.* 2018;16:1–28. doi: 10.1186/s12951-018-0334-5. [DOI] [PMC free article] [PubMed] [Google Scholar]
12. Marambio-Jones C., Hoek E.M.V. A review of the antibacterial effects of silver nanomaterials and potential implications for human health and the environment. *J. Nanopart. Res.* 2010;12:1531–1551. doi: 10.1007/s11051-010-9900-y.
13. Argueta Figueroa L., Arenas-Arocena M.C., Díaz-Herrera A.P., García-Benítez S.V., García-Contreras R. Propiedades antimicrobianas y citotóxicas de un adhesivo de uso ortodóncico adicionado con nanopartículas de plata. *Mundo Nano. Rev. Interdiscip. Nanocienc. Nanotecnol.* 2018;12:1. doi: 10.22201/ceiich.24485691e.2019.22.62550.
14. Ge L., Li Q., Wang M., Ouyang J., Li X., Xing M.M.Q. Nanosilver particles in medical applications: Synthesis, performance, and toxicity. *Int. J. Nanomed.* 2014;9:2399–2407. doi: 10.2147/IJN.S55015.
15. Cheng G., Dai M., Ahmed S., Hao H., Wang X., Yuan Z. Antimicrobial drugs in fighting against antimicrobial resistance. *Front. Microbiol.* 2016;7:470. doi: 10.3389/fmicb.2016.00470.
16. Betts J.W., Hornsey M., La Ragione R.M. *Novel Antibacterials: Alternatives to Traditional Antibiotics.* 1st ed. Volume 73. Elsevier Ltd.; Amsterdam, The Netherlands: 2018.
17. Yaqoob A.A., Umar K., Ibrahim M.N.M. Silver nanoparticles: Various methods of synthesis, size affecting factors and their potential applications—A review. *Appl. Nanosci.* 2020;10:1369–1378. doi: 10.1007/s13204-020-01318-w. [DOI] [Google Scholar]
18. Ferdous Z., Nemmar A. Health impact of silver nanoparticles: A review of the biodistribution and toxicity following various routes of exposure. *Int. J. Mol. Sci.* 2020;21:2375. doi: 10.3390/ijms21072375.



How to cite this article:

Manoj Kumar et al. Jcpr.Human, 2026; Vol. 22 (3): 6-12.

Conflict of Interest Statement:

The authors have no conflicts of interest to declare.

This is an open access article under the terms of the Creative Commons Attribution-NonCommercial-NoDerivs License, which permits use and distribution in any medium, provided the original work is properly cited, the use is non-commercial and no modifications or adaptations are made.